Chapter 4

Recent Progress of Plasma CVD for Structure Controlled Growth of Single-Walled Carbon Nanotubes

Toshiaki Kato and Rikizo Hatakeyama

Additional information is available at the end of the chapter

http://dx.doi.org/10.5772/51966

1. Introduction

One-dimensional single-walled carbon nanotubes (SWNTs) are potential materials for future nanoelectronics. Since the electronic and optical properties of SWNTs strongly depend on their structure, such as diameter and chirality, the selective synthesis of SWNTs with desired structure is a major challenge in nanotube science and applications. SWNT growth was first achieved by arc discharge in 1993. Several growth techniques have been developed since then, including laser ablation and chemical vapor deposition (CVD). Since it is possible to grow SWNTs at a specific position on a substrate by patterning a catalyst, CVD has attracted much attention in nanoelectronics applications. In general, CVD can be divided into two types: thermal CVD [1-4] and plasma CVD [5-7]. Due to the strong electric fields in plasma sheaths, nanotubes grown by plasma CVD tend to have an individually-and vertically-free standing shape [5,8-10]. Thermal CVD decomposes carbon source gases using thermal energy. In contrast, in plasma CVD, the source gas decomposition is effectively carried out by electron impact with no additional thermal energy; hence, the growth temperature is significantly lower compared to that of thermal CVD. Despite these benefits of plasma CVD, it is difficult to control the structure of SWNTs by plasma CVD because there are many unknown factors in plasma, such as ion density, ion energy, radical species, radical densities, and sheath electric field, which restrict the potential application of plasma CVD in nanotube science. Based on our studies, SWNT growth by plasma CVD has been significantly improved in recent years. In this chapter, we give a brief overview of recent progress in SWNT growth by plasma CVD.

2. Freestanding single-walled carbon nanotube growth

The potential of plasma CVD for nanotube growth was first demonstrated by Ren et al. in 1998 [5]. Vertically- and individually-aligned multi-walled carbon nanotubes (MWNTs) are

grown by plasma CVD. Since carbon nanotubes (CNTs) grown by thermal CVD are known to form a spaghetti-like entangled shape, the well-aligned growth of CNTs by plasma CVD makes it an attractive CNT-growth method that may solve the integration issue in CNT-based nanoelectronics. However, plasma CVD is limited to the production of MWNTs; SWNTs, which have superior electrical and optical characteristics compared with MWNTs, have not been successfully produced by plasma CVD. The growth of SWNTs by plasma CVD was first reported by our group in 2003 [11, 12]. SWNTs are grown by plasma CVD using a zeolite as a catalyst support. Zeolites are nanoporous materials known to maintain small catalyst particle sizes on their rough surfaces, even under high-temperature conditions. Thus, certain plasma effects might enhance catalyst particle aggregation during plasma CVD, which could be the main reason why SWNTs could not be grown by plasma CVD. It is thought that catalyst particle aggregation is enhanced due to high-energy ions attacking the catalyst. In general, ions in plasma are accelerated through the potential drop between space potentials in the plasma and substrate biases. The minimum value of this potential drop is determined by the electron temperature in the plasma. Thus, low electron-temperature plasma can significantly decrease the energy of ions arriving at the substrate. Since the diffusion region in plasma is known to have very low electron temperatures, we used the diffusion plasma to decrease the energy of ions attacking the catalyst to below a few eV. SWNT growth under the diffusion plasma region occurs on a flat substrate without using catalyst support materials [13, 14]. Thus, the critical element promoting catalyst aggregation is high-energy ion bombardment. Interestingly, SWNTs grown by diffusion-plasma CVD have the well-aligned freestanding form, i.e., all SWNTs are individually- and vertically-standing on the flat substrate. Figures 1a–d show a typical scanning electron microscope (SEM) image (Figure 1a), low-magnification (Figure 1b) and high-magnification (Figure 1c) transmission electron microscope (TEM) images, and Raman scattering spectra (Figure 1d) of freestanding SWNTs. Relatively high-quality SWNTs were grown with the individually freestanding form, and this alignment can be obtained by the plasma-sheath electric field. Based on numerical calculation, the rotation energy of the dipole moment in SWNTs is much higher than the thermal energy, which disturbs the tube alignment [14]. This indicates that individual SWNTs can be aligned along the electric field. Owing to their unique as-grown state, it is possible to directly detect photoluminescence (PL) spectra from the as-grown freestanding SWNTs on the substrate (Figure 1e) [15]. This is a remarkable advantage for optoelectrical applications and fundamental studies toward chirality control, which will be discussed later.

3. Growth kinetics of SWNTs in plasma CVD

In this section, we report a crucial finding of remarkable etching reaction of SWNTs during the plasma CVD, and key parameters for such etching reaction are also revealed with a numerical analysis of the experimentally established SWNT-growth equation. A reactive ion etching model is also developed to explain the etching reaction of SWNTs in plasmas[16].

http://dx.doi.org/10.5772/51966

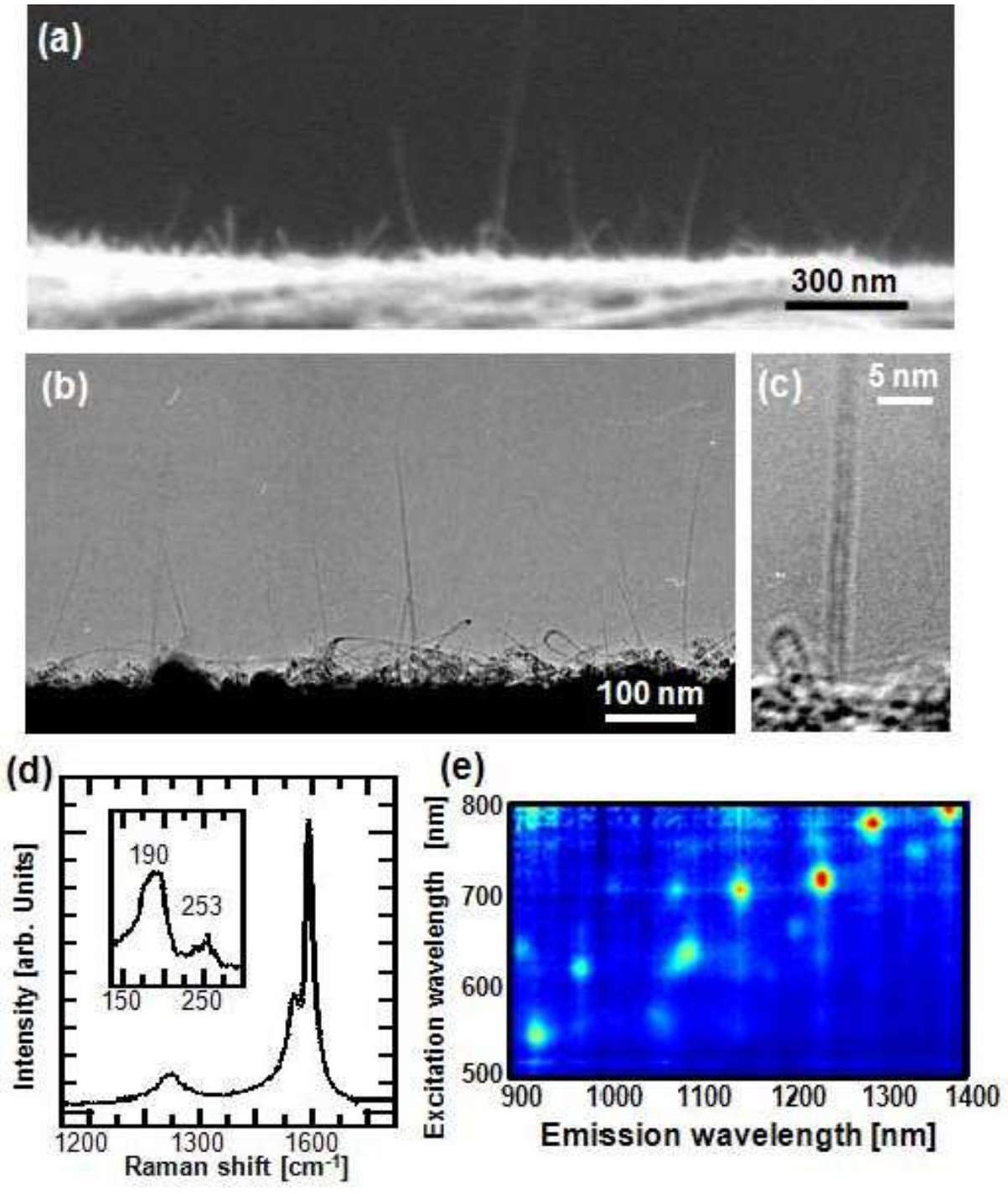

Figure 1. (a) SEM and (b) (c) TEM images of freestanding individual SWNTs. (d) Raman scattering spectrum of freestanding individual SWNTs. Inset of (d) is emphasis of the RBM region. (e) PLE map obtained from as-grown freestanding SWNTs without any dispersion process.

Figures 2a and b presents typical Raman scattering spectra of SWNTs as a function of growth time (t_g). Raman scattering spectroscopy has been known as one of the powerful tools to characterize the SWNTs structure such as diameter, chirality, quality, and so on. In addition to these structural information, the absolute value of G-band intensity (I_G) at 1593

cm^{-1} originating from a graphite nature in the SWNTs is sometimes utilized to discuss the amount of SWNTs. As information of the amount of SWNTs, therefore, we utilize the absolute value of I_G measured under the almost same experimental conditions; laser power: ~ 0.2 $mW/\mu m^2$, laser wavelength: 488 nm, laser spot size: 4 μm^2, accumulation time: 60 sec. When radio-frequency power (P_{RF}) is 40 W, I_G gradually increases with an increase in t_g (Figure 2a). On the other hand, I_G suddenly decreases when the growth time is longer than 50 sec under the 100 W P_{RF} condition (Figure 2b). These results indicate that the growth kinetics of SWNTs is strongly influenced by the plasma conditions, and several specific factors in plasmas cause the strong etching of SWNTs as shown in Figure 2b.

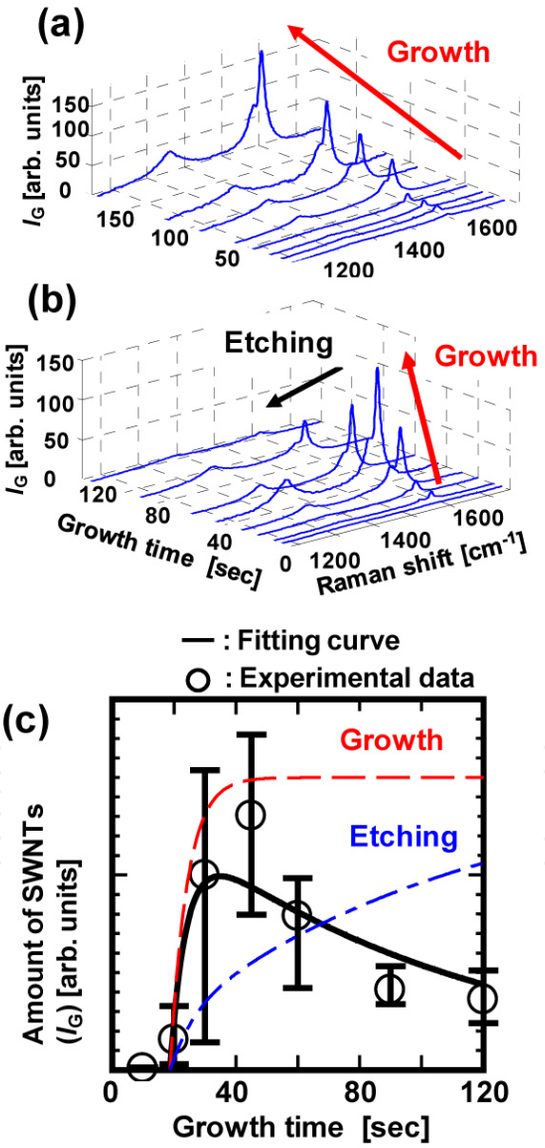

Figure 2. Raman spectra of SWNTs as a function of t_g. (a) P_{RF} = 40 W and (b) P_{RF} = 100 W, respectively. (c) The comparison between the experimental data and fitting curve of Eq. 1.

http://dx.doi.org/10.5772/51966

In the case of the thermal CVD, it has been reported that the growth kinetics of SWNTs can be expressed with a following equation (normal equation) [17]. $I_G = I_0[1-\exp\{-(t_g - \Delta t)/\tau_{gro}\}]$, where I_0, Δt, and τ_{gro} denote saturated I_G, incubation time, and relaxation time of the growth, respectively. Our experimental results of damage free growth (Figure 2a) well match with this equation, which denotes our estimation of SWNTs amount with I_G is reliable. However, there is obviously no formula which can describe the growth kinetics including the etching effect as described in Figure 2b. On purpose to express this phenomenon, therefore, we assume that the growth mode can be described with a following balance equation: $I_G = G(t_g) - E(t_g)$, where $G(t_g)$ and $E(t_g)$ are growth and etching functions, respectively. When the etching effect is weak and negligible, the growth kinetic has to be described with the above-mentioned normal equation, which means that $G(t_g)$ is the same as the normal equation. One of the most important points in this study is how to describe $E(t_g)$. Since carbon atoms are etched out only when atoms or molecules attach themselves to the carbon atoms in SWNTs, the probability of the etching reaction can be simplified in terms of an adsorption reaction. The Langmuir's adsorption isotherm is known as one of the most basic ones, and to be expressed by the following form: $d\theta/dt = \alpha P(1-\theta)$, where θ, t, α, and P indicate the percentage of covered area, reaction time, adsorption efficiency, and pressure of adsorbate, respectively. Actually, the Langmuir's equation has been utilized in the wide range of fundamental scientific studies to understand chemical adsorption reactions. In our study, θ corresponds to the etched area against the area of the graphite sheet of SWNTs, *i.e.* $\theta = E(t_g)/G(t_g)$. Since the solution of the Langmuir's equation is $\theta(t_g) = 1-\exp(-t_g/\tau_{etc})$, where $\tau_{etc} = 1/\alpha P$ is the relaxation time of the etching reaction, $E(t_g)$ results in the following equation: $E(t_g) = G(t_g)\{1-\exp(-t_g/\tau_{etc})\}$. According to the above mentioned equations, an advanced growth equation can be established as

$$I_G = I_0\left[1-\exp\left\{\frac{-(t_g-\Delta t)}{\tau_{gro}}\right\}\right]\left\{\exp\left(\frac{-t_g}{\tau_{etc}}\right)\right\} \quad (1)$$

Figure 2c shows a comparison between the experimental result of Figure 2b and fitting curve with Eq. (1). The fitting curve gives good agreement with the experimental result, indicating that the advanced equation established enables us to discuss a more detailed correlation between plasma parameters such as ion energy U_i and species density and growth parameters such as and etching efficiency ($k = 1/(\tau_{etc}-\tau_{gro})$).

Based on the advanced growth Eq. (1), we attempt to understand effects of U_i coming to the substrate during the SWNT growth. Figure 3a gives a counter plot of I_G as functions of t_g and U_i. Since U_i is determined by a potential drop between the plasma and substrate, the substrate bias voltage is changed to adjust U_i. When U_i is fairly low (~ 1 eV), I_G gradually increases and saturates with an increase in t_g. The similar tendency can also be found under the condition of U_i = 30 eV. When U_i = 10 eV and over 50 eV, on the other hand, a sudden decrease of I_G can be found after the specific t_g (t_g >150 ~ 200 sec). This decrease of I_G indicates that the etching reaction arises at these specific energy window of ions as similar to the

result in Figure 2b. The I_G/I_D plot also supports the evidence of etching reaction in such a specific energy range, where I_D is D-band intensity around 1350 cm^{-1} in Raman spectroscopy. Only under the U_i condition of 10 eV and > 50 eV, the SWNTs quality remarkably decreases independently of t_g (Figure 3b). These lead us to conclude that several significant damages are likely caused via energetic ions ranging around 10 eV and over 50 eV.

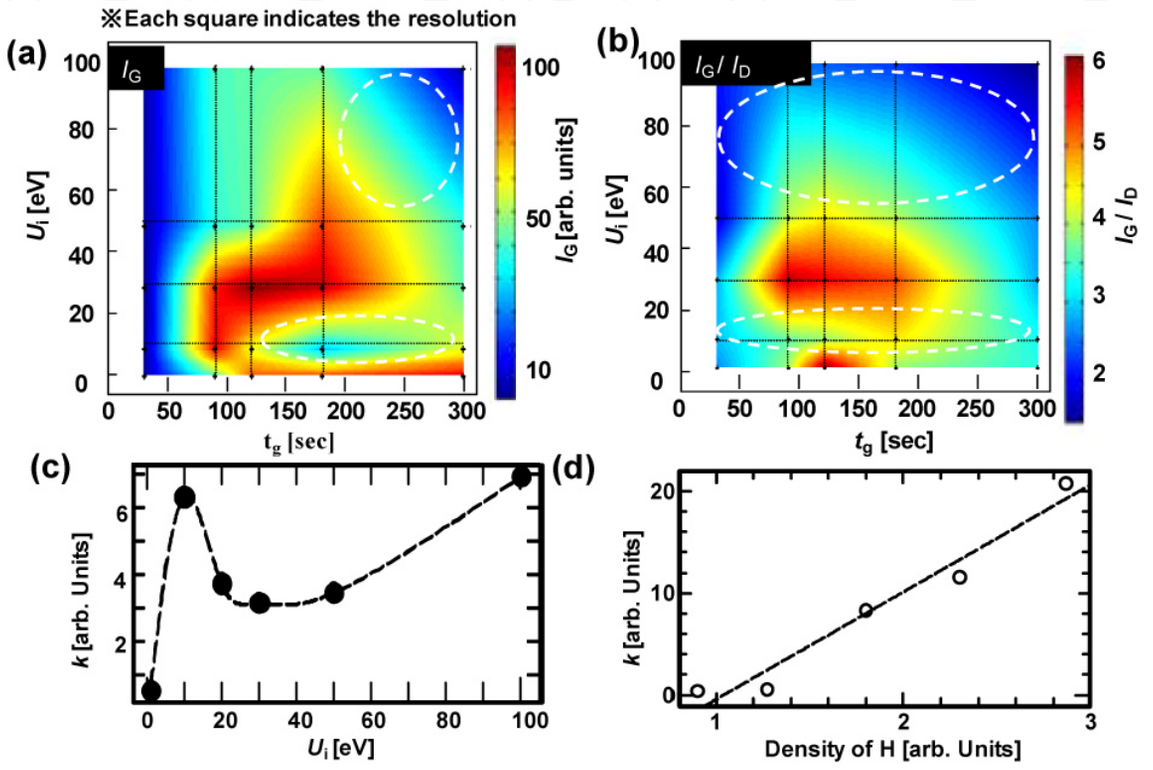

Figure 3. (a), (b) Contour plot of I_G (a) and I_G/I_D (b) as functions of U_i and t_g. Each dot indicates the condition, where experiments have been done. For visuall help, all of data between each dot are computationally compensated. (c) Etching efficiency k as a function of U_i. (d) Etching efficiency k as a function of relative density of H.

A further quantitative and practical analysis is also performed upon the fitting of experimental results with the advanced growth equation (Eq. 1). Figure 3c shows a plot of estimated k under the different U_i condition. As similar to the result in Figures 3a and b, the clear increment of k is recognized under the specific energy condition of U_i = 10 eV and > 50 eV.

In addition to the ions, there are many kinds of factors causing significant impacts on the structure of SWNTs in hydrocarbon plasmas. Especially, the density of radicals is much higher than that of ions in reactive plasmas. Thus we attempt to reveal a correlation of k with several radical densities. The relative densities of radicals are measured by an Actinomery method with optical emission spectroscopy (OES). When k is plotted as a function of H density, it is surprising that a clear liner correlation is found as displayed in Figure 3d. Although the dependence of H on etching reactions has already been mentioned by several groups without any direct measurement of H density, our time-evolution results combined

with the systematical H-density measurement afford more direct evidence for the primal factor determining k during the growth of SWNTs.

Based on the above mentioned experimental results, a consistent reactive ion-etching model can be established as follows. In our study, the etching efficiency k is expressed by the following equation

$$k = 1/(\tau_{etc} - \tau_{gro}) \approx 1/\tau_{etc} = \alpha P \quad (2)$$

The linear dependence of k on H density shown in Figure 3d indicates that the density of H corresponds to in Eq. 2. Since the density of H is kept constant during the experiment of ion energy effects, on the other hand, the supplied amount of etching elements (P) must be constant. Hence, the variation of k depending on U_i (Figure 3c) originates from the difference of α. Under the specific U_i condition, the carbon-carbon bond is considered to be broken, and the efficiency of adsorption between the carbon and etching element (H) resultantly comes to increase. After all, the direct factor causing the etching of SWNTs is the H, and the specific energy of ions enhances those etching reactions by changing the adsorption efficiency between the carbon and hydrogen atoms.

4. Structure-controlled growth of SWNTs

The structure of SWNTs, including diameter and chirality, strongly influences their electrical and optical properties; therefore, it is important to precisely control the structure of SWNTs. Here, we discuss recent progress in the structure-controlled growth of SWNTs by plasma CVD.

4.1. Diameter control

The band gap is known to be inversely proportional to tube diameter; thus, controlling the tube diameter is very important for electrical and optical applications. Here, we present our experimental results for diameter tuning of SWNTs based on gas-phase control in plasma CVD [18].

Figures 4a–d show photoluminescence-excitation (PLE) maps of as-grown SWNTs produced at different gas pressures. Note that all PLE measurements were carried out immediately after the growth process to prevent the freestanding SWNTs from forming bundles, which cause significant PL changes [15]. Peaks in the PLE map at high growth pressures (Figure 4a) appeared in the range of long excitation and emission wavelengths. The peak positions shifted to the region of short excitation and emission wavelengths with decreasing growth pressure (Figures 4b–d). Since each peak corresponds to a different chirality in the sample, and smaller-diameter SWNTs appeared in the shorter wavelength region, the peak-position shifts in the PLE map indicate that the diameter distribution of SWNTs is strongly influenced by growth pressure. Thus, lower pressure results in smaller SWNT diameters. This di-

ameter dependence on the growth pressure is also reflected in Raman scattering spectra of SWNTs grown at different growth pressures. Figure 4e shows that peak positions of the radial breathing mode (RBM) clearly shifted from higher to lower wavenumbers with increasing growth pressure. The RBM peak position and the SWNT diameter are known to have a close correlation, $\omega = 248/d$ [19], where ω and d are the RBM peak position (cm^{-1}) and diameter (nm), respectively. This result is fairly consistent with the PLE result shown in Figures 4a–d. The typical pressure range where SWNTs can be grown is from 30 Pa to 650 Pa and depends on the P_{RF} used for the plasma generation. Although the absolute intensity of the G-band in Raman scattering spectra decreased in the low- or high-pressure range, the G-band to D-band ratio was almost constant. This indicates that the quality of SWNTs should be independent of the pressure range, whereas the density of SWNTs depends on the pressure. When we increased the input P_{RF}, it was possible to grow SWNTs, even below 30 Pa, indicating that a lack of hydrocarbon supply is significant under low-pressure conditions. Hence, an additional input P_{RF} is required to increase the density of active species used for the growth of SWNTs.

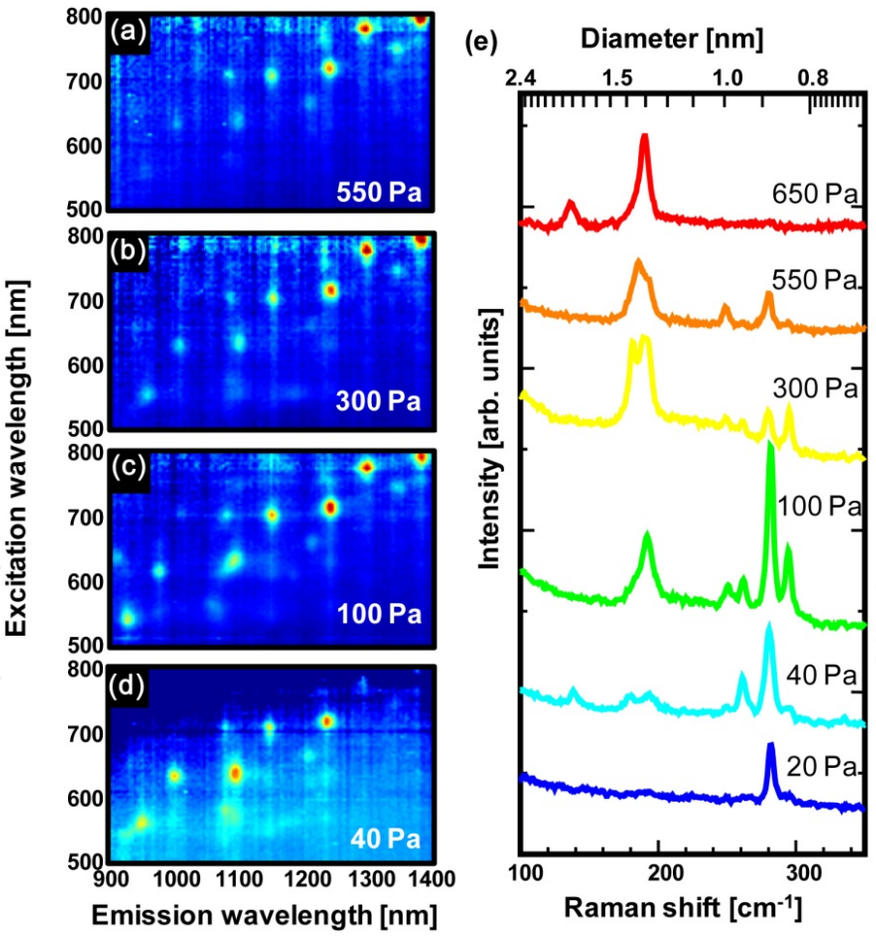

Figure 4. (a-d) PLE maps of as-grown freestanding SWNTs grown under different pressures, (a) 550 Pa, (b) 300 Pa, (c) 100 Pa, and (d) 40 Pa. (e) Growth pressure dependency of RBM in Raman scattering spectra of as-grown freestanding SWNTs.

http://dx.doi.org/10.5772/51966

Since the pressure during the heating and growth were the same in our growth process, the process pressure affected both the heating and the growth process. Based on this systematic investigation, we believe that the catalyst particle size increased due to aggregation after high-pressure annealing, which resulted in the growth of large-diameter SWNTs. The density of reactive hydrocarbon radicals and ions should increase under higher growth pressure conditions. Under high carbon supply conditions, a small catalyst can be deactivated by an oversupply of hydrocarbons, causing the population of small-diameter SWNTs to decrease. Therefore, the heating pressure is an important parameter that controls the catalyst particle size distribution, which directly influences the diameter of SWNTs. The pressure during plasma CVD is also important for a narrow SWNT diameter distribution [18].

4.2. Selective growth of semiconducting SWNTs

Field effect transistors (FETs) are one of the most promising applications of SWNTs. Although the high mobility and flexibility of SWNTs films can provide lots of opportunities to be utilized in various kinds of industrial applications, the low on/off current ratio in SWNT FETs caused by the mixture of metallic and semiconducting SWNTs restricts the practical use of SWNTs in FET applications. Recent progress in chemical separation enables us to fabricate good devices with on/off ratio: ~10^4 and effective gate mobility: ~ 52 cm^2/Vs. However, impurities and defects are sometimes introduced in chemically treated nanotubes during the separation process, which significantly decreases the device performance. Since as-grown SWNTs maintain the original high-quality with low impurity concentration, the selective growth of semiconducting SWNTs is desirable. Dai *et al*. reported the preferential growth of semiconducting SWNTs by plasma CVD. Although several similar reports with plasma CVD and thermal CVD have also been reported, the elucidation of this selective growth is still an open question and further investigations are needed. Here we discuss our recent findings that show a clear correlation between the performance of semiconducting devices fabricated by plasma CVD and their mean diameter [20], which might lead to a possible explanation for the preferential growth of semiconducting SWNTs by plasma CVD.

Figure 5a shows typical Raman scattering spectra of SWNTs grown under different growth temperatures. The high graphite (G)-peak to defect (D)-peak ratio indicates that the quality of SWNTs is comparable to other conventional CVD grown SWNTs. The RBM in a lower wave number region in Raman spectra exhibits the clear down shift with an increase in the growth temperature. The mean diameter of SWNTs is found to increase with growth temperature. This seems to be due to the catalyst particle size effect. Higher growth temperatures cause particle aggregation and result in the increase of the particle size, which can produce larger diameter SWNTs. A clear dependence is obtained from the plot of on current (I_{on}) vs. on/off ratio (I_{on}/I_{off}) as a function of SWNTs growth temperature. The on/off ratio of each device clearly decreases with a decrease in the growth temperature (Figure 5b). The concentration of the working devices, which have on/off ratios greater than 5, is counted and plotted as a function of the growth temperature (Figure 5c). Noticeably, the working device concentration is only 2.5 % in the case of 600 ºC (smaller diameter SWNTs), whereas

more than 90 % of the devices work in the case of 800 ºC (larger diameter SWNTs). The density of SWNTs grown under the different growth temperatures is almost the same.

In order to explain the dependence of the working device concentration on the SWNT diameter, devices were irradiated by an Ar plasma, and a defect formation rate is estimated from the current change before and after the plasma treatment. In the case of small diameter SWNTs devices, the on/off ratio does not change, and on and off currents significantly decrease after the Ar plasma irradiation, whereas the on/off ratio increases with an increase in the Ar plasma irradiation time and the off current depression is significant compared to that of the on current in the case of large diameter SWNTs devices. Based on these results, the following model can be developed to explain the dependence of the working device concentration on the diameter. Due to the curvature effect, small diameter SWNTs are more unstable than large diameter ones. Hence, both metallic and semiconducting SWNTs are easily deformed by the Ar plasma irradiation without any difference in the tube metallicity. On the other hand, in the weak curvature range, the dependence of the defect formation rate on a unique metallicity appears, which might correlate with the reactivity, binding energy between carbon and carbon, and healing process. This model is consistent with the selective etching of metallic SWNTs by gas phase reaction, which was previously reported. Further detailed studies relating to the selective damage of metallic SWNTs might provide the possible answer for the preferential growth of semiconducting SWNTs by plasma CVD.

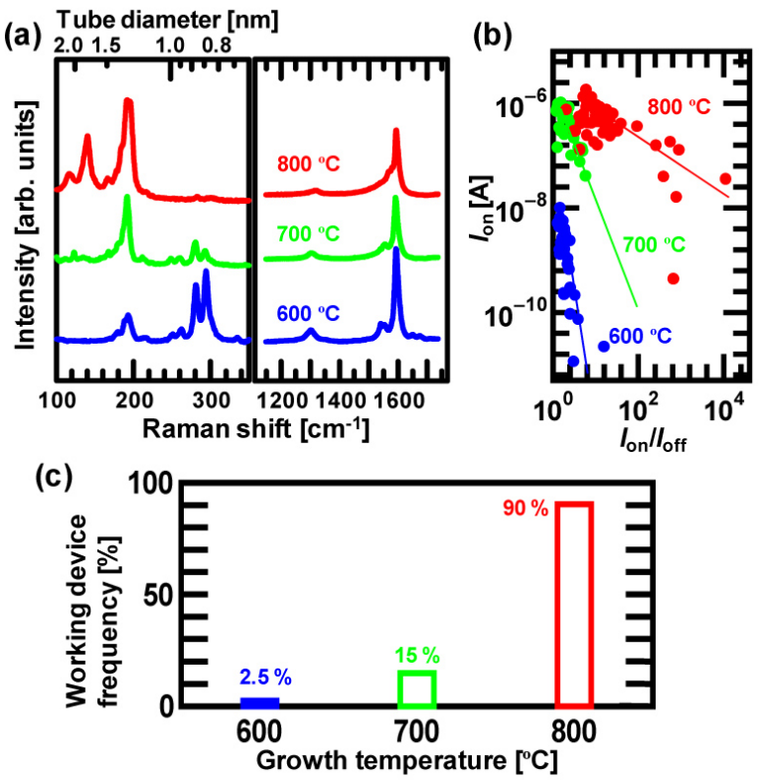

Figure 5. (a) Raman scattering spectra of SWNTs grown at different growth temperatures (laser excitation energy: 1.96 eV). (b) I_{on}-I_{on}/I_{off} plot of TFT devices with SWNTs grown at different growth temperatures. (c) Histogram of working device concentration of TFT devices with SWNTs grown at different growth temperatures.

http://dx.doi.org/10.5772/51966

4.3. Narrow-chirality distributed growth of SWNTs

The chirality of SWNTs directly determines their electronic and optical properties; thus, selective synthesis of SWNTs with desired chiralities is a major challenge in nanotube science and applications. In this session, we demonstrate the recent progresses of narrow chirality distributed growth of SWNTs by plasma CVD based on different two approaches, which focus on catalytic reaction and gas phase reaction.

4.3.1. Catalytic reaction control

Narrow chiratliy distributed growth of SWNTs is one of the most critical issue in the scientific field of SWNTs production stage. Some progress has been made with silica-supported CoMo [21] and zeolite-supported FeCo [22] catalysts. FeRu [23] and FeNi [24] catalysts have also been developed to achieve narrow chirality distributions. Interestingly, all syntheses resulting in narrow chirality distributions have involved magnetic catalysts. The main obstacle to research on intrinsic magnetic properties of SWNTs is residual ferromagnetic catalyst particles; thus, SWNT growth with nonmagnetic catalysts is beneficial. Despite recent improvements in SWNT growth with nonmagnetic catalysts [25-28], diameter and chirality (n,m) distribution control with nonmagnetic catalysts is still required for fundamental studies and a variety of applications [29].

Based on this background, we attempto to grow SWNTs with narrow chirality distributions using nonmagnetic catalyst [30, 31]. PLE mapping was used to assign (n,m) of SWNTs grown from the Au catalyst at different H_2 concentrations (Figures 6a–c). The total pressure was kept at 50 Pa by adjusting the pumping rate of the rotary pump throughout this experiment. Lower H_2 concentrations (0 and 3 sccm) led to larger diameters and wider (n,m) distributions with (6,5), (7,5), (7,6), (8,4), (8,6), and (8,7) (Figures 6a and b). On the other hand, the 7-sccm H_2 concentration yielded the narrowest (n,m) distribution with a dominant peak corresponding to the (6,5) tube (Figure 6c). The UV-Vis-NIR optical absorbance spectra of Au-plasma CVD SWNTs grown at the 7-sccm H_2 flow rate showed one dominant peak in the first van Hove E_{11} range (900–1400 nm) corresponding to SWNTs with (6,5) chirality (Figure 6d). Since clear metallic SWNT peaks were not observed in the UV-Vis-NIR spectra (Figure 6d), the concentration of metallic SWNTs was lower than that of the generally grown SWNTs. This is the first result showing narrow chirality distributions for SWNTs grown from a nonmagnetic catalyst [31].

To elucidate the effects of Au and plasma CVD on the narrow chirality distribution, other combinations of catalysts and CVD methods were systematically investigated. Based on the PLE analysis, SWNTs grown by the Fe catalyst with plasma CVD (Fe-plasma CVD) did not show a clear correlation between the H_2 flow rate and the chirality distribution, which was broader than that of SWNTs grown by Au-plasma CVD. This indicates that H_2-assisted Au catalyzation is a critical factor for achieving narrow chirality distributions, which is in good agreement with theoretical predictions. The first-principle calculation by Yazyev *et al.* reveals that coinage metals, such as Cu, Ag, and Au, produce narrow chirality distributions [32]. Ding *et al.* have reported that the SWNT diameter is larger on the surfaces of Fe, Co, and Ni particles than on Cu, Pd, and Au particles because of the different bond energies on

the catalyst surfaces [33]. Based on these theoretical models, we can explain the effect of H_2-assisted Au catalyzation on the narrow chirality distirbution as follows. Since the binding energy of hydrocarbons on the Au surface is much weaker than on the Fe surface, it is difficult to achieve cap formation for large-diameter Au catalysts [33]. Additonal H_2 also enhances the etching of the carbon precursor from the catalyst surface, which strongly suppresses the growth of large-diameter SWNTs; hence, the chirality distribution of SWNTs grown from the Au catalyst should be narrower than those grown from the Fe catalyst. The stability of the cap structure is a possible reason why the (6,5) tube was dominant in the small-diameter Au-plasma CVD SWNTs. The number of cap structures, which satisfies the isolated pentagon rule, is highly limited for small-diameter SWNTs, and (6,5) is known to have a stable cap structure in this diameter range [22]. A comparison between Au-plasma CVD and Au-thermal CVD was also carried out. Although the chiraity distribution became relatively narrow for SWNTs grown by Au-thermal CVD under appropriate H_2 concentrations, it was much broader than that of SWNTs grown by Au-plasma CVD. Comparison of the Au-plasma CVD and Au-thermal CVD processes showed that there were two significant differences in the SWNT growth conditions: growth temperature and incubation time. The lower limit of growth temperature for Au-plasma CVD was 700 °C, which was lower than that of Au-thermal CVD by 50 °C. The initial SWNT growth occurred 1 min after the growth substrate was exposed to the plasma for Au-plasma CVD, whereas 15 min were required for the growth of SWNTs with Au-thermal CVD. These results suggest that the low-temperature and short-time growth with Au-plasma CVD prevents aggregation of catalyst particles during SWNT growth, which suppresses the growth of large-diameter SWNTs and results in a narrow chiratliy distribution.

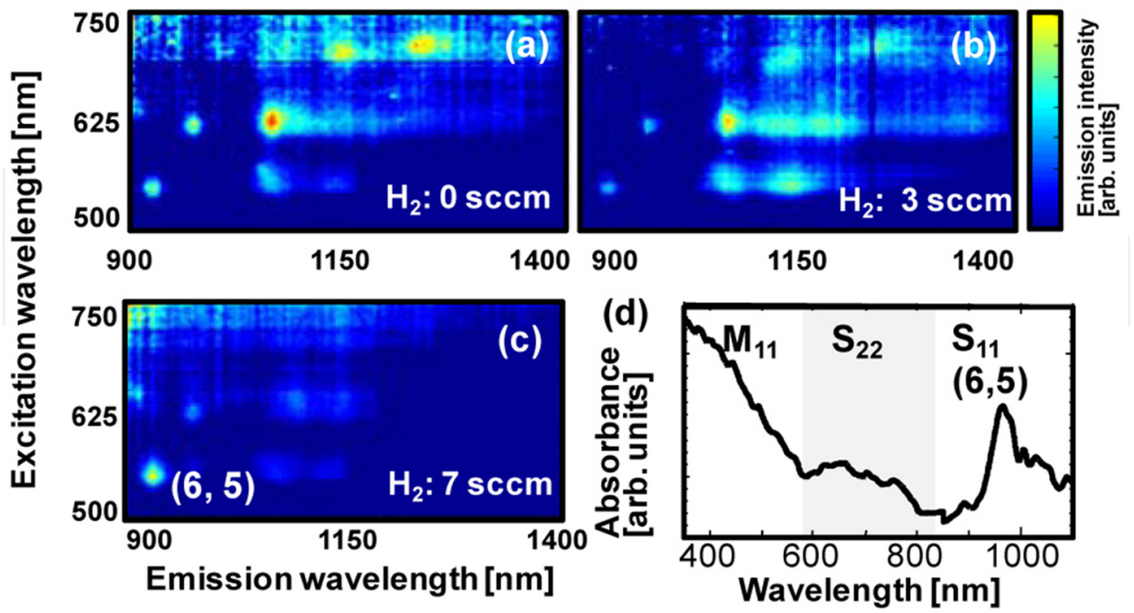

Figure 6. (a) PLE maps of SWNTs from Au catalyst by plasma CVD at (a) 0-sccm, (b) 3-sccm, and (c) 7-sccm H_2 flow rates, respectively. (d) UV-vis-NIR spectrum of SDS-dispersed SWNTs from Au catalyst at 7-sccm H_2 flow rate.

http://dx.doi.org/10.5772/51966

4.3.2. Gas phase reaction control

Recent progress in the in-situ TEM observation during the SWNT growth revealed that metal-catalyzed SWNT growth is initiated by the formation of a carbon cap structure on the surface of a catalytic nanoparticle with a certain incubation time (t_i) [34]. Although the detailed mechanism in this incubation period is still argued, it is expected that there might be correlations between the t_i and SWNT structures such as the d_t and chirality. When we assume that the t_i of the small d_t (or specific chirality) SWNTs is shorter than that of the larger (or other chiralities) one, it should be possible to selectively grow the narrow-d_t (or -chirality) distributed SWNTs by strictly controlling the t_g at their initial growth stage. Chemical vapor deposition (CVD), thermal CVD and plasma CVD, is one of the most promising SWNT production methods, which has advantages such as a large scale production and a direct site-assigned growth. In the case of thermal CVD, the SWNT growth gradually starts and stops after the initiation of feeding and pumping the hydrocarbon gas, respectively (Figure 7a). The growth time in thermal CVD includes some uncertainness, which makes it difficult to be used for a precise growth time control. In the case of plasma CVD, on the other hand, reactive ions and radicals are main species for the nanotubes growth, and the SWNT growth is carried out only when a plasma is generated. This suggests that the growth time can be controlled by timing an electric power supply used for the plasma generation (Figure 7b), and the precise t_g control on the order of micro second is possible in plasma CVD. Based on this strategy, we attempt to grow the narrow-d_t and -chirality distributed short SWNTs by precisely adjusting the t_g with time programmed-plasma CVD (TP-PCVD).

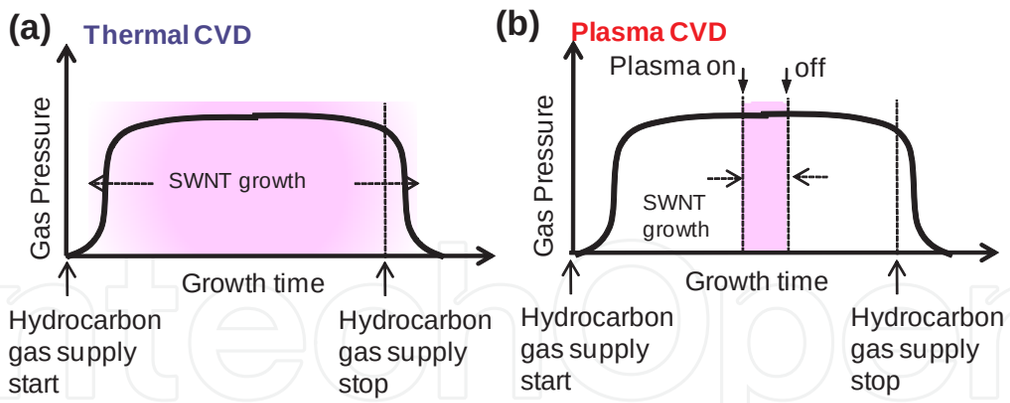

Figure 7. (a) (b) Time evolution of thermal (a) and plasma (b) CVD.

In order to analyze the chirality distribution of the short SWNTs in detail, we carry out the PLE map analysis. It is to be noted that since our plasma CVD grown SWNTs take on the freestanding form due to the strong electric field in the plasma sheath area during their growth, it is possible to observe PL signals from as-grown SWNTs on a substrate [15]. All the PLE measurements are carried out immediately after the growth to prevent SWNTs from forming thin bundles, which leads to causing the PL intensity change by exciton energy transfer between each tube [15]. From the density estimation of SWNTs with the direct

TEM observations, it is confirmed that abundant SWNTs exist in the area where the PLE measurement is carried out. Thus, the PLE map gives us macroscopic information in each sample. Figures 8a-c show the PLE maps of the as-grown SWNTs as a function of t_g. It is found that the d_t distribution just after the incubation (2 sec) is relatively narrow and the main diameter is about 0.8 nm with (6, 5), (7, 5), (7, 6), (8, 4), and (9, 2) dominant chiralities (Figure 8a). Then, the relatively large d_t (0.95 nm) SWNTs ((8, 6) and (9, 4)) initiate their growth at 5 sec (Figure 8b). The larger d_t SWNTs of (8, 7) are finally grown at 10 sec, where the chirality and d_t distributions are broad (Figure 8c). The small end of the d_t does not change, whereas the large end increases with an increase in the t_g. In more detail, when we plot the t_i as a function of the d_t, a clear dependence is obtained (Figure 9). It is to be noted that the t_i of each chirality is defined as the t_g when a clear PL signal is firstly observed (Figures 8a-c). The t_i increases with an increase in the tube diameter, which supports the validity of our basic concept.

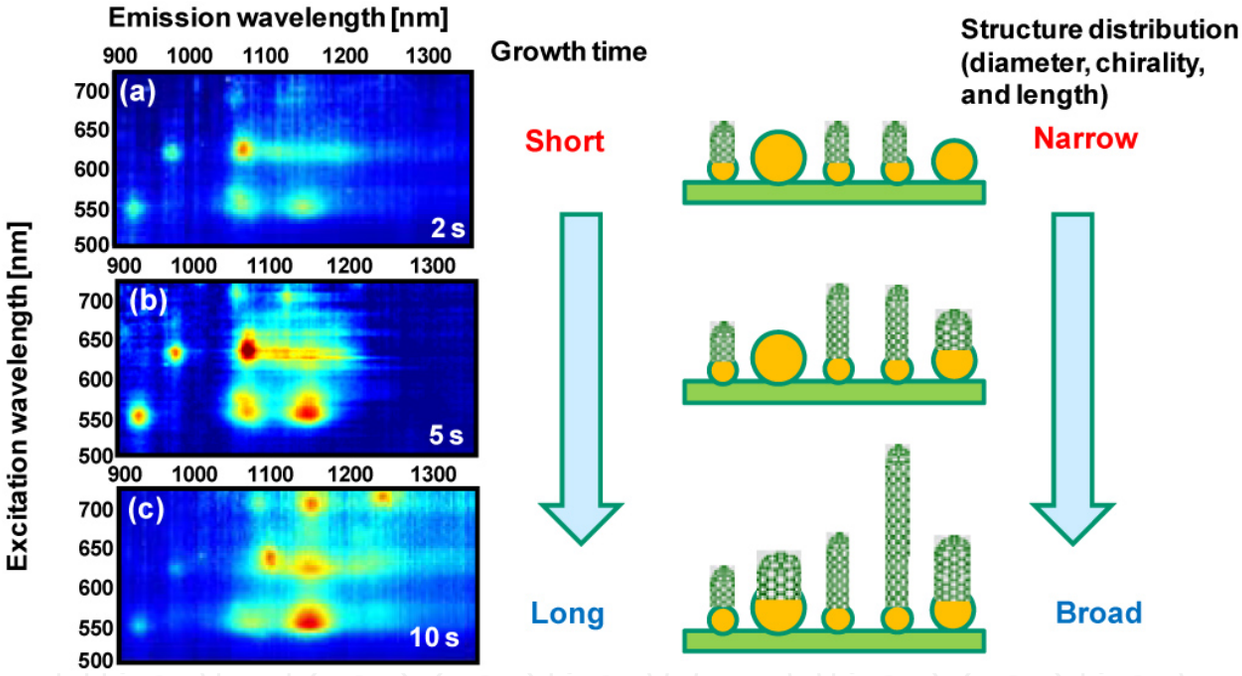

Figure 8. Chirality and diameter distribution of SWNTs as a function of growth time. (a)(b)(c) PLE-map of SWNTs produced by different growth time, which is 2 sec (a), 5 sec (b), and 10 sec (c).

To further narrow the initial d_t and chirality distributions, we adjust the other growth conditions. Figure 10 shows the PLE map dependence on the growth temperature of SWNTs grown for the very short growth time (2 sec). Interestingly, when we decrease the growth temperature down to 600 ºC the chirality distribution is very narrowed, and (7,6) and (8,4) SWNTs are predominantly grown (Figure 10c). At the lower growth temperature (≤ 580 ºC), SWNTs could not be grown for the very short growth time (2 sec). However, similar narrow-chirality distributed SWNTs are grown by extending the growth time until 15 sec. This indicates that the t_i for each d_t and chirality is sensitive to the growth temperature. It should be also emphasized that the chirality distribution just after the t_i is always narrow independ-

http://dx.doi.org/10.5772/51966

ent of other growth parameters. The narrow-chirality distributed SWNTs growth by TP-PCVD is reproducibly obtained. This is the first result of the direct growth of the short-length SWNTs with a narrow-chirality distribution [35].

The most important factor for the narrow-chirality distributed growth of short SWNTs by TP-PCVD is to control the d_t dependence on t_i for each chirality SWNT. If each t_i largely varies depending on the d_t or chirality of SWNT, it is possible to more selectively grow the specific chirality SWNTs by adjusting the growth time. As shown in Figure 10, the growth temperature is one of the key factors to cause the t_i variation for each d_t SWNT. The cap formation process might be one of the critical reasons for this temperature dependence. The central part of the graphene sheet formed on the top of catalyst surface has to lift off the catalytic particle for the growth of SWNTs. This can only happen if the kinetic energy per area at the interface between the graphene sheet and the catalyst (E_{kin}) is high enough to overcome the work of adhesion per area of graphite toward the catalytic particle (W_{ad}) ($E_{kin} > W_{ad}$)[36]. Small tubes have lower W_{ad}[37]. Since the E_{kin} should be proportional to the growth temperature, the producible type of SWNTs under the low growth temperature condition can be highly selected compared with that in the higher growth temperature.

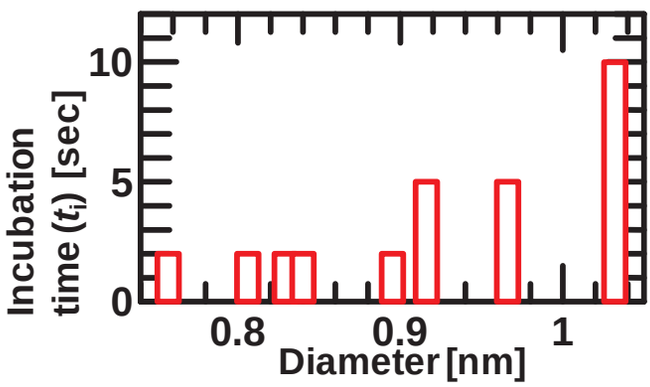

Figure 9. Plot of incubation time as a function of tube diameter.

As we have discussed above, the growth temperature is one of the key parameters to realize the narrow-chirality distribution of SWNTs by TP-PCVD. In order to realize the further precise control of the d_t and chirality distribution, it is inevitable issue to reveal the critical factor, which causes the d_t dependence on the t_i. The catalyst particle-size variation during the heating process might be one possibility. If the catalyst aggregation is enhanced during the growth process, the chirality distribution also changes. To investigate this issue, we carry out the PLE mapping measurement of SWNTs grown for the different preheating time. After heating the substrate up to 620 ºC, the temperature is kept for certain time (0 sec, 30 sec, and 60 sec), and then similar TP-PCVD is carried out. If the catalyst particle size distribution varies during the heating process and this is the critical factor of the d_t dependence on t_i, clear differences should appear in the PLE map of SWNTs grown under the different preheating conditions. In any preheating time, however, the d_t and chirality distribution does not show obvious changes. This indicates that the catalyst size distribution is almost the

same during the short time growth (Figures 8a-c), and its effect is negligible for the d_t dependence on t_i (Figure 9).

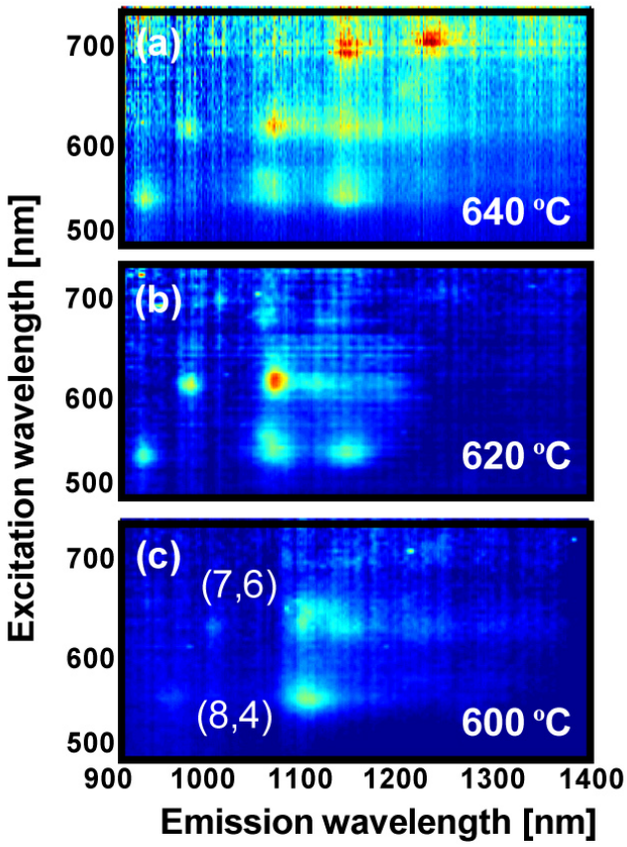

Figure 10. Growth temperature dependence of the PLE-maps of SWNTs grown for very short growth time (2sec). The growth temperature of (a), (b), and (c) is 640 ºC, 620 ºC, and 600 ºC, respectively.

The other possibility to cause the d_t dependence on the t_i is a supersaturation time difference. Since the SWNTs growth is carried out following a supersaturation of carbons in a catalyst, it is expected that the small catalysts are rapidly supersaturated with carbon atoms prior to the case of the large catalysts. To confirm this effect, we carry out the PLE map measurement of SWNTs grown under the low hydrocarbon supply condition. If the supersaturation time difference is the critical factor to cause the d_t dependence on the t_i, the selectivity of d_t or chirality should be improved by decreasing the hydrocarbon supply. The amount of the hydrocarbon supply is controlled by adjusting P_{RF} used for the plasma generation. The t_i clearly increases up to 20 sec by decreasing the amount of hydrocarbon supply (P_{RF} = 25 W), which should be caused by the longer supersaturation period of carbons in the catalyst at their initial growth stage. However, various kinds of chirality species of SWNTs equally start their growth and the selective growth of narrow-d_t or -chirality distributed SWNTs are not observed under this low hydrocarbon supply condition. Although the t_i for whole SWNTs is sensitive to the hydrocarbon supply, the selectivity of d_t or chirality is found to be conducted by the other factors. A simple estimation based on the carbon atom

http://dx.doi.org/10.5772/51966

numbers also supports the validity of this explanation. The soluble carbon atoms in a typical 1 nm Fe catalyst (Fe_{50}) is about 26 ~ 27 [38]. On the other hand, the number of carbon atoms constructing a 1 nm d_t and 100 nm length SWNT is about 2.35×10^4. Judging from this carbon atom numbers, it is difficult to selectively achieve the supersaturation only for the d_t = 0.8 nm with 100 nm length SWNT prior to the d_t = 0.95 nm SWNT (Figure 9).

5. Conclusions

Recent progress in SWNT growth was presented, with a special emphasis on plasma CVD. Due to the strong plasma-sheath electric field, it is possible to grow freestanding individual SWNTs by plasma CVD. Based on the time-evolution study and the detailed plasma parameter measurements, the growth kinetics of SWNTs in plasma CVD were well established. The concentration of semiconducting SWNTs in FET devices can be increased by tuning the mean diameter of SWNTs, and this effect is attributable to selective damage of metallic SWNTs during plasma CVD. Moreover, narrow chirality-distributed growth of SWNTs were also achieved by different two approaches. Au catalyzed plasma CVD with appropriate amount of hydrogen addition can realize preferential gorwth of (6,5) SWNTs. The narrow chirality distributed growth of SWNTs were also demonstrated with precise incubation time control by time-programmed plasma CVD.

Author details

Toshiaki Kato and Rikizo Hatakeyama

Department of Electronic Engineering, Tohoku University, Sendai, Japan

References

[1] Kong, J., Cassell, A. M., & Dai, H. (1998). Recent progress of plasma CVD for structure controlled growth of single-walled carbon nanotubes . *Chemical Physics Letters*, 567 EOF-574 EOF.

[2] Maruyama, S., Kojima, R., Miyauchi, Y., Chiashi, S., Kohno, M., & Low, . (2002). Recent progress of plasma CVD for structure controlled growth of single-walled carbon nanotubes . *Chemical Physics Letters*, 229 EOF.

[3] Dai, H., Rinzler, A. G., Nikolaev, P., Thess, A., Colbert, D. T., Smalley, R. E., & Single, . (1996). Recent progress of plasma CVD for structure controlled growth of single-walled carbon nanotubes . *Chemical Physics Letters*, 471 EOF-475 EOF.

[4] Tibbetts, G. G. (1992). Recent progress of plasma CVD for structure controlled growth of single-walled carbon nanotubes . *Carbon*, 30(3), 399-406.

[5] Ren, Z. F., Huang, Z. P., Xu, J. W., Wang, J. H., Bush, P., Siegal, M. P., & Provencio, P. N. (1998). Recent progress of plasma CVD for structure controlled growth of single-walled carbon nanotubes . *Science*, 282(6), 1105-1107.

[6] Chhowalla, M., Teo, K. B. K., Ducati, C., Rupesinghe, N. L., Amaratunga, G. A. J., Ferrari, A. C., Roy, D., Robertson, J., & Milne, W. I. (2001). Recent progress of plasma CVD for structure controlled growth of single-walled carbon nanotubes . *Journal of Applied Physics*, 90(10), 5308-5317.

[7] Delzeit, L., Nguyen, C. V., Stevens, R. M., Han, J., & Meyyappan, M. Growth of Carbon Nanotubes by Thermal and Plasma Chemical Vapor Deposition Processes and Applications in Microscopy. Nanotechnology (2002). , 13(3), 280-284.

[8] Hirata T., Satake N., Jeong G.-H., Kato T., Hatakeyama R., Motomiya K., and Tohji K., Magnetron-Type Radio-Frequency Plasma Control yielding Vertically Well-Aligned Carbon Nanotube Growth. (2003). *Applied Physics Letters*, 83(6), 1119-1121.

[9] Bower, C., Zhu, W., Jin, S., Zhou, O., & Plasma, . (2000). Recent progress of plasma CVD for structure controlled growth of single-walled carbon nanotubes . *Applied Physics Letters*, 77(6), 830-832.

[10] Merkulov, V. I., Melechko, A. V., Guillorn, M. A., Lowndes, D. H., & Simpson, M. L. (2001). Recent progress of plasma CVD for structure controlled growth of single-walled carbon nanotubes . *Applied Physics Letters*, 79(18), 2970-2972.

[11] Kato, T., Jeong, G., , H., Hirata, T., Hatakeyama, R., Tohji, K., Motomiya, K., & Single, . (2003). Recent progress of plasma CVD for structure controlled growth of single-walled carbon nanotubes . *Chemical Physics Letters*, 422 EOF.

[12] Kato, T., Jeong, G., , H., Hirata, T., Hatakeyama, R., & Tohji, K. Recent progress of plasma CVD for structure controlled growth of single-walled carbon nanotubes . Japanese Journal of Applied Physics(2004). A) LL1280., 1278.

[13] Kato, T., Hatakeyama, R., & Tohji, K. Diffusion Plasma Chemical Vapor Deposition Yielding Freestanding Individual Single-Walled Carbon Nanotubes on a Silicon-Based Flat Substrate. Nanotechnology (2006). , 17(9), 2223-2226.

[14] Kato, T., & Hatakeyama, R. Recent progress of plasma CVD for structure controlled growth of single-walled carbon nanotubes . Chemical Vapour Deposition (2006). , 12(6), 345-352.

[15] Kato, T., & Hatakeyama, R. (2008). Recent progress of plasma CVD for structure controlled growth of single-walled carbon nanotubes . *Journal of the American Chemical Society*, 130(25), 8101-8107.

[16] Kato, T., & Hatakeyama, R. (2008). Recent progress of plasma CVD for structure controlled growth of single-walled carbon nanotubes . *Applied Physics Letters*, 031502 EOF.

[17] Chiashi, S., Ph, D., thesis, Univ., & of, . Tokyo (2005).

[18] Kato, T., Kuroda, S., & Hatakeyama, R. (2011). Recent progress of plasma CVD for structure controlled growth of single-walled carbon nanotubes . *Journal of Nanomaterials*.

[19] Jorio A., Saito R., Hafner J. H., Lieber C. M., Hunter M., McClure T., Dresselhaus G., and Dresselhaus M. S. Structural (n,m) Determination of Isolated Single-Wall Carbon Nanotubes by Resonant Raman Scattering. Physical Review Letters 2001; 86(6) 1118–1121.

[20] Kato, T., & Hatakeyama, R. Recent progress of plasma CVD for structure controlled growth of single-walled carbon nanotubes . Journal of Nanotechnology 2010; (2010).

[21] Kitiyanan, B., Alvarez, W. E., Harwell, J. H., & Resasco, D. E. (2000). Recent progress of plasma CVD for structure controlled growth of single-walled carbon nanotubes . *Chemical Physics Letters*, 497 EOF-503 EOF.

[22] Miyauchi, Y., Chiashi, S., Murakami, Y., Hayashida, Y., & Maruyama, S. (2004). Recent progress of plasma CVD for structure controlled growth of single-walled carbon nanotubes . *Chemical Physics Letters*, 198 EOF.

[23] Li, X., Tu, X., Zaric, S., Welsher, K., Seo, W. S., Zhao, W., & Dai, H. (2007). Recent progress of plasma CVD for structure controlled growth of single-walled carbon nanotubes . *Journal of the American Chemical Society*, 129(51), 15770-15771.

[24] Chiang, W. H., & Sankaran, M. R. Linking Catalyst Composition to Chirality Distributions of As-Grown Single-Walled Carbon Nanotubes by Tuning NixFe1−x Nanoparticles. Nature Materials (2009). , 8(11), 882-886.

[25] Zhou, W., Han, Z., Wang, J., Zhang, Y., Jin, Z., Sun, X., Zhang, Y., Yan, C., & Li, Y. (2006). Recent progress of plasma CVD for structure controlled growth of single-walled carbon nanotubes . *Nano Letters*, 6(12), 2987-2990.

[26] Takagi, D., Homma, Y., Hibino, H., Suzuki, S., Kobayashi, Y., & Single, . (2006). Recent progress of plasma CVD for structure controlled growth of single-walled carbon nanotubes . *Nano Letters*, 6(12), 2642-2645.

[27] Takagi, D., Kobayashi, Y., Hibino, H., Suzuki, S., & Homma, Y. (2008). Recent progress of plasma CVD for structure controlled growth of single-walled carbon nanotubes . *Nano Letters*, 8(3), 832-835.

[28] Bhaviripudi S., Mile E., Steiner III S. A., Zare A. T., Dresselhaus M. S., Belcher A. M., and Kong J. CVD Synthesis of Single-Walled Carbon Nanotubes from Gold Nanoparticle Catalysts. Journal of the America Chemical Society 2007; 129(6) 1516–1517.

[29] , Y., Lehtinen, P. O., Foster, A. S., & Nieminen, R. M. (2004). Recent progress of plasma CVD for structure controlled growth of single-walled carbon nanotubes . *New Journal of Physics*, 68 EOF.

[30] Ghorannevis, Z., Kato, T., Kaneko, T., & Hatakeyama, R. Growth of Single-Walled Carbon Nanotubes from Nonmagnetic Catalysts by Plasma CVD. Japanese Journal of Applied Physics (2010). BA01-1-4.

[31] Ghorannevis, Z., Kato, T., Kaneko, T., Hatakeyama, R., & Narrow, . (2010). Recent progress of plasma CVD for structure controlled growth of single-walled carbon nanotubes . *Journal of the American Chemical Society*, 132(28), 9570-9572.

[32] Yazyev, O. V., & Pasquarello, A. Recent progress of plasma CVD for structure controlled growth of single-walled carbon nanotubes . Physical Review Letters (2008).

[33] Ding, F., Larsson, P., Larson, J. A., Ahuja, R., Duan, H., Rosen, A., & Bolton, K. (2008). Recent progress of plasma CVD for structure controlled growth of single-walled carbon nanotubes . *Nano Letters*, 8(2), 463-468.

[34] Hofmann, S., Sharma, R., Ducati, C., Du, G., Mattevi, C., Cepek, C., Cantoro, M., Pisana, S., Parvez, A., Cervantes-Sodi, F., Ferrari, A. C., Dunin-Borkowski, R., Lizzit, S., Petaccia, L., Goldoni, A., & Robertson, J. (2007). Recent progress of plasma CVD for structure controlled growth of single-walled carbon nanotubes . *Nano Letters*, 7(3), 602-608.

[35] Kato, T., & Hatakeyama, R. (2010). Recent progress of plasma CVD for structure controlled growth of single-walled carbon nanotubes . *ACS Nano*, 4(12), 7395-7400.

[36] Ding, F., Bolton, K., & Rosen, A. Recent progress of plasma CVD for structure controlled growth of single-walled carbon nanotubes . Journal of Physical Chemistry B (2004). , 108-17369.

[37] Kanzow, H., Lenski, C., Ding, A., & Single, . (2001). Recent progress of plasma CVD for structure controlled growth of single-walled carbon nanotubes . *Physical Review B*.

[38] Ding, F., Larsson, P., Larsson, J. A., Ahuja, R., Duan, H., Rosen, A., & Bolton, K. Recent progress of plasma CVD for structure controlled growth of single-walled carbon nanotubes . Nano Lett. (2008). , 8-463.